Electronic Supplementary Information for:

Near-infrared fluorescent probe reveals decreased mitochondrial polarity during mitophagy

Xiaoyi Li,[ab] Xiaohua Li,[a]* and Huimin Ma[ab]*

[a] Beijing National Laboratory for Molecular Sciences, Key Laboratory of Analytical Chemistry for Living Biosystems, Institute of Chemistry, Chinese Academy of Sciences, Beijing 100190, China.
E-mail: lixh@iccas.ac.cn; mahm@iccas.ac.cn

[b] University of Chinese Academy of Sciences, Beijing 100049, China.

1 Apparatus and reagents

NMR spectra were conducted on Bruker Fourier 300, Bruker Avance III HD 400 or 600 spectrometer in MeOD-d_4 or DMSO-d_6 (Cambridge Isotope Laboratories). High-resolution electrospray ionization mass spectrometry (HR-ESI-MS) was performed on an APEX IV FTMS instrument (Bruker, Daltonics). UV-vis absorption spectra were recorded on a UV-2600 spectrophotometer (Shimadzu, Japan) in 1-cm quartz cells. Fluorescence spectra were acquired on a Hitachi F-4600 spectrophotometer in 1 × 1 cm quartz cells with both excitation and emission slit widths of 10 nm and a PMT voltage of 400 V. MTT [3-(4,5-dimethyl-2-thiazolyl)-2,5-diphenyl-2H-tetrazolium bromide] analyses were conducted on a microplate reader (BIO-TEK Senergy HT, U.S.A.). Confocal fluorescence images were performed on an FV 1200-IX83 confocal laser scanning microscope (Olympus, Japan) and image processing was carried out with Olympus software (FV10-ASW).

Unless otherwise specified, all reagents, including metal ions, thiols, H_2O_2, and other chemicals, were purchased from J&K Scientific Ltd., Beijing Chemical Plant or Sigma-Aldrich and used as received. Rhodamine 123 (Rh 123) and ER-Tracker Green (ER Green) were ordered from Thermo Fisher. Carbonyl cyanide m-chlorophenylhydrazone (CCCP) and rapamycin was obtained from MedChem Express. MitoTracker Green FM (Mito Green), LysoTracker Green DND-26 (DND-26), human cervical cancer cells (HeLa), human fetal lung fibroblast 1 (HFL-1), human liver carcinoma cells (HepG2)，human normal liver cells (L-O2), Dulbecco's modified Eagle's media (DMEM), Ham's F-12K (Kaighn's) medium, trypsin/EDTA solution, were purchased from KeyGEN BioTECH Co., Ltd, Nanjing, China. The preparation of reactive oxygen species and their concentration determinations were following the reported method (Li et al, *Anal. Chem.* **2017**, *89*, 5519). Ultrapure water (over 18 MΩ·cm) produced by a Milli-Q reference system (Millipore) was used throughout the whole experiments.

2 Synthesis of fluorescent probe HXPI-P and HXPI-M

As depicted in Scheme S1, HXPI-P, HXPI-M and HXPI-E were synthesized in a single step.

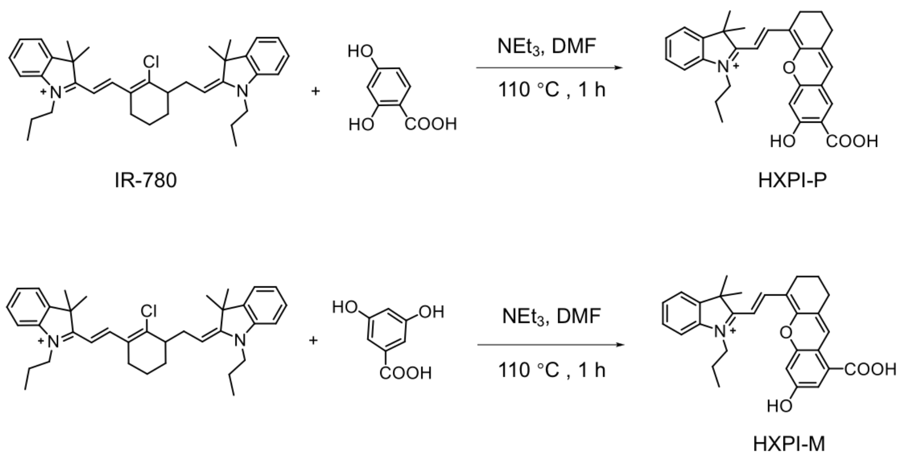

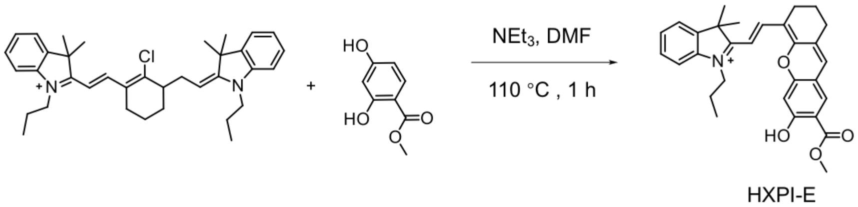

Scheme S1. Synthetic procedure of HXPI-P, HXPI-M and HXPI-E.

Synthesis of HXPI-P. 2,4-Dihydroxybenzoic acid (69 mg, 0.45 mmol) and IR-780 (150 mg, 0.23 mmol) were dissolved in dry DMF (5.0 mL) and stirred at room temperature. Triethylamine (0.20 mL) was added slowly and the reaction mixture was warmed up to 110 °C under argon protection. After 1 h, the solvent was evaporated under reduced pressure and the residue was purified by silica gel chromatography (CH_2Cl_2/CH_3OH, 20:1), affording HXPI-P (31 mg, 30%) as blue solid. ^{1}H NMR of HXPI-P (400 MHz, DMSO-d_6; Fig. S1) δ 8.53 (d, *J* = 16.0 Hz, 1H), 7.97 (s, 1H), 7.69(d, *J* = 8.0 Hz, 2H), 7.57 (d, *J* = 8.0 Hz, 1H), 7.47 (t, *J* = 8.0 Hz, 1H), 7.36 (t, *J* = 8.0 Hz, 1H), 6.67 (s, 1H), 6.39 (d, *J* = 12.0 Hz, 1H), 4.28 (t, *J* = 8.0 Hz, 2H), 2.70-2.65 (m, 4H), 1.83-1.78 (m, 4H), 1.74 (s, 6H), 0.98 (t, *J* = 8.0 Hz, 3H). ^{13}C NMR of HXPI-P (150 MHz, CD_3OD; Fig. S2) δ 176.1, 171.0, 162.2, 164.9, 159.9, 154.6, 144.0, 140.5, 140.2, 133.0, 128.9, 127.2, 125.3, 124.3, 120.9, 116.2, 112.8, 112.1, 110.9, 101.7, 100.4, 49.0, 44.6, 27.0, 25.4, 22.1, 19.3, 18.8, 8.67. HR-ESI-MS: *m/z* calcd for $[C_{29}H_{29}NNaO_4]^+$, 478.1994; found, 478.1989 (Fig. S3).

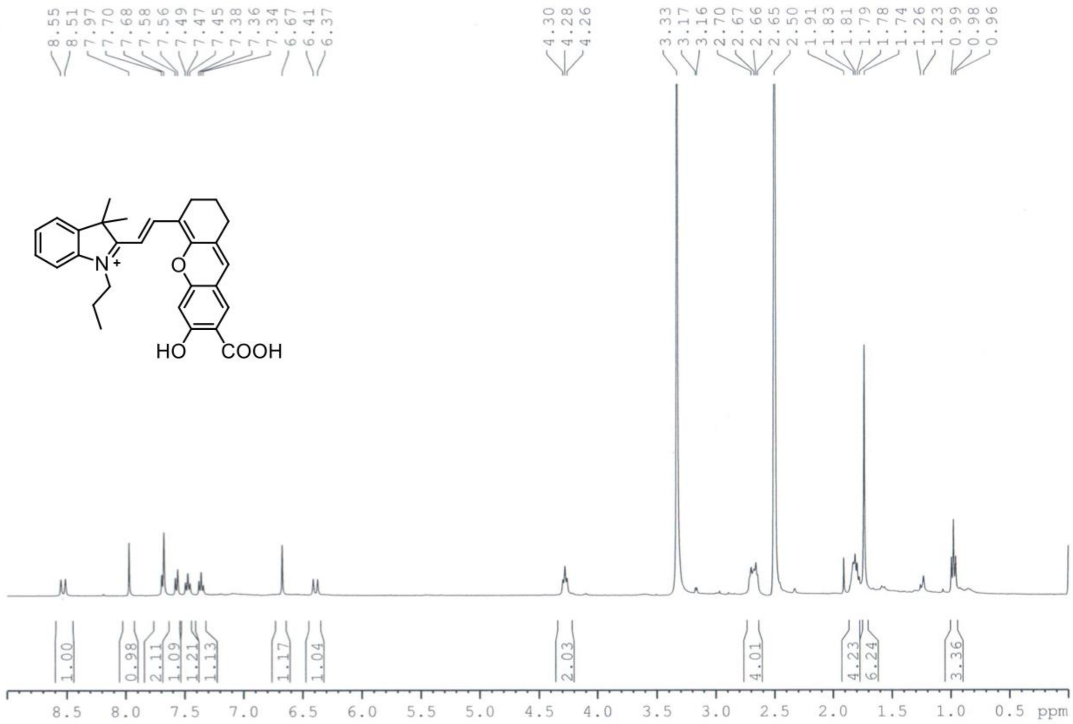

Fig. S1 ^{1}H NMR spectrum of HXPI-P (400 MHz, DMSO-d_6, 298 K)

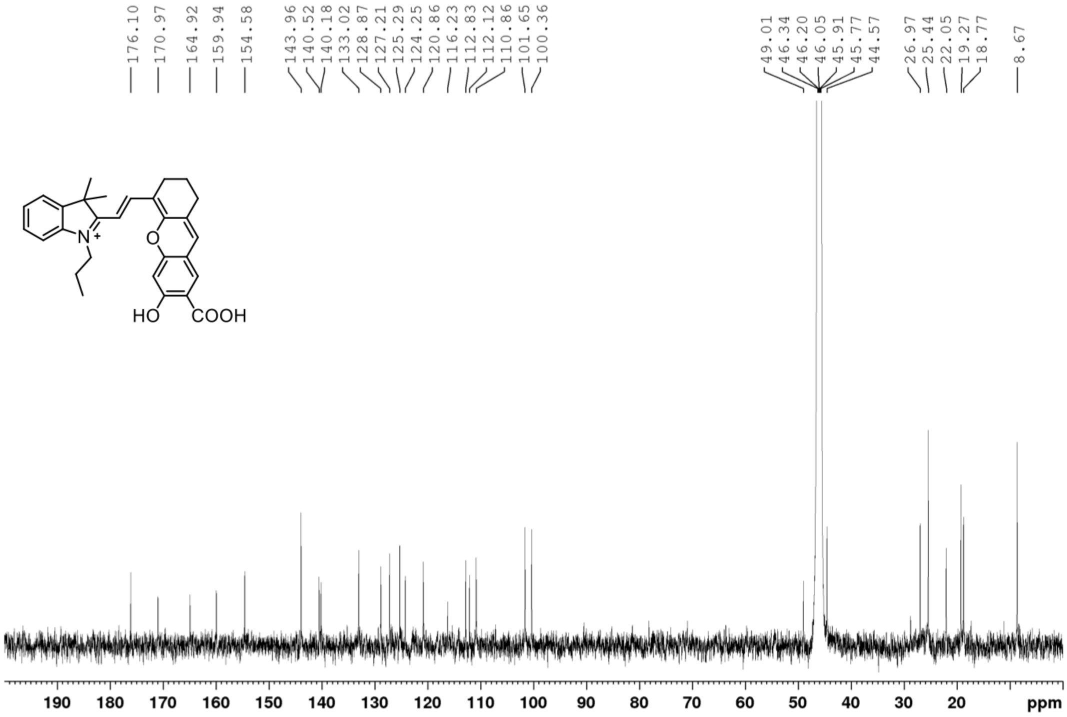

Fig. S2 ^{13}C NMR spectrum of HXPI-P (150 MHz, CD_3OD, 298 K).

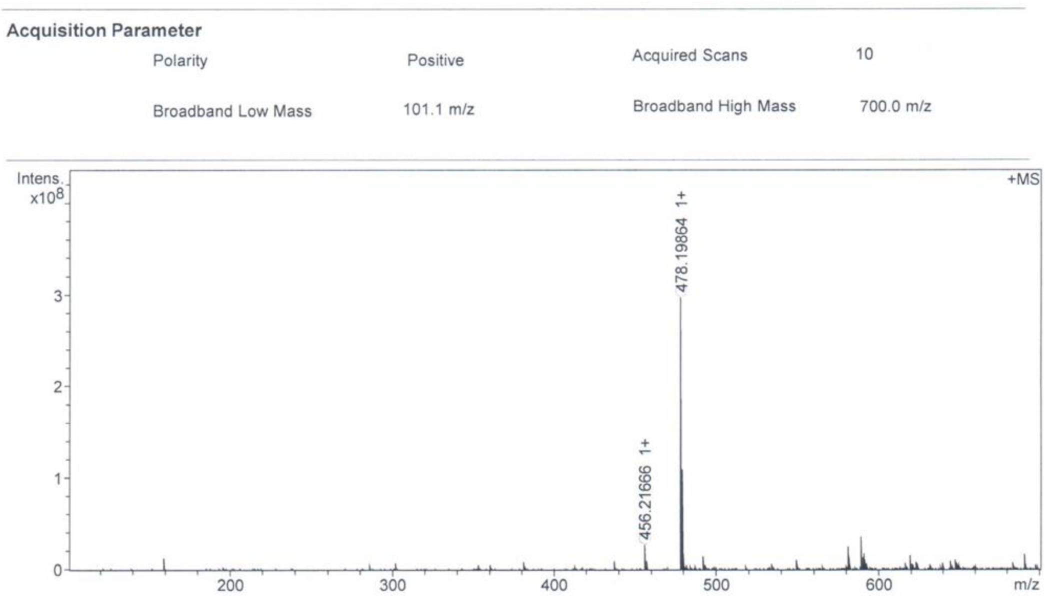

Fig. S3 HR-ESI-MS of HXPI-P

Synthesis of HXPI-M. HXPI-M was obtained by the condensation of 3,5-dihydroxybenzoic acid and IR-780 with same procedure as mentioned above. Yield: 50%. ^{1}H NMR of HXPI-M (400 MHz, CD_3OD; Fig. S4) δ 8.72 (d, *J* = 13.2 Hz, 1H), 8.31 (s, 1H), 7.67(m, 1H), 7.57 (m, 2H), 7.46-7.43 (m, 2H), 6.97 (s, 1H), 6.52 (d, *J* = 13.6 Hz, 1H), 4.35 (m, 2H), 2.78-2.71 (m, 4H), 1.95 (m, 4H), 1.83 (s, 6H), 1.09 (m, 3H). ^{13}C NMR of HXPI-M (150 MHz, CD_3OD; Fig. S5) δ 178.1, 167.2, 160.7, 160.4, 159.9, 155.0, 145.1, 142.1, 141.6, 131.7, 128.9, 127.8, 127.2, 122.4, 116.61, 116.59, 114.4, 114.1, 112.7, 105.3, 103.8, 50.7, 46.3, 29.1, 26.8, 23.6, 20.9, 20.3, 10.2. HR-ESI-MS: *m/z* calcd for $[C_{29}H_{30}NO_4]^+$, 456.2169; found, 456.2169 (Fig. S6).

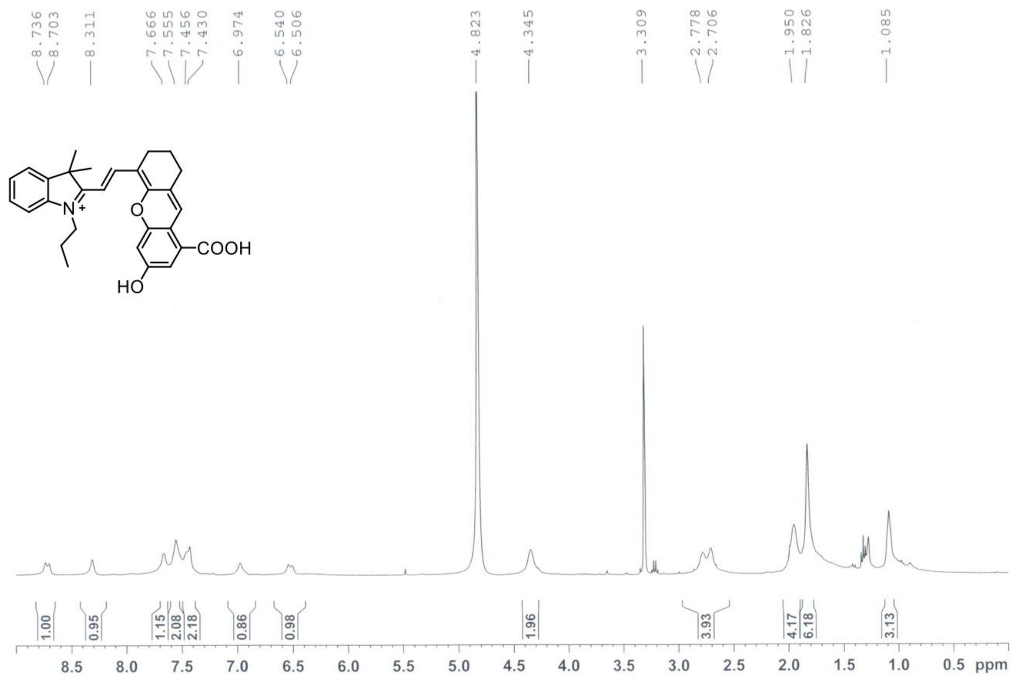

Fig. S4 ^{1}H NMR spectrum of HXPI-M (400 MHz, CD_3OD, 298 K)

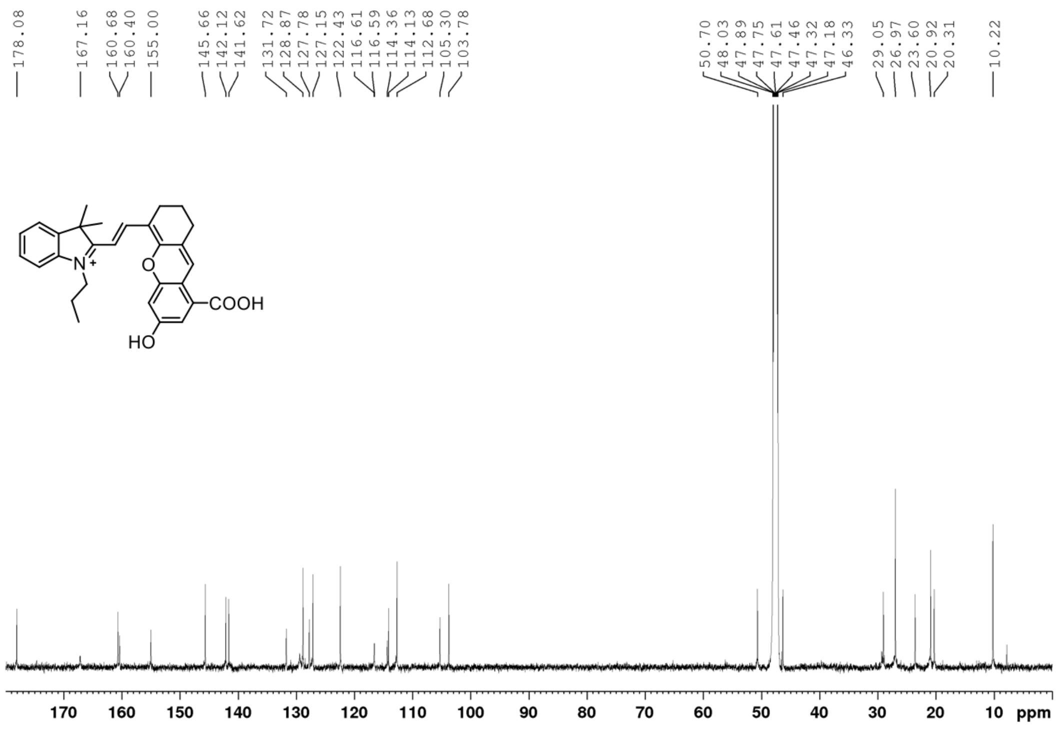

Fig. S5 ^{13}C NMR spectrum of HXPI-M (150 MHz, CD_3OD, 298 K).

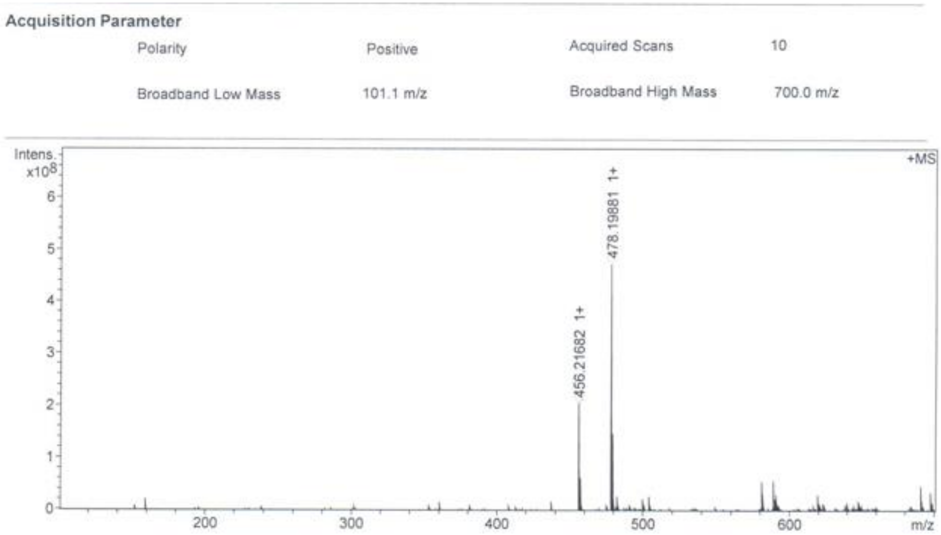

Fig. S6 HR-ESI-MS of HXPI-M.

Synthesis of HXPI-E. HXPI-E was obtained by the condensation of methyl 2,4-dihydroxybenzoate and IR-780 with the same procedure as mentioned above. Yield: 70%. ^{1}H NMR of HXPI-E (300 MHz, CD_3OD; Fig. S7) δ 8.69 (m, 1H), 7.97 (m, 1H), 7.72(m, 2H), 7.56 (m, 2H), 7.22 (d, J = 3.3 Hz, 1H), 6.89 (m, 1H), 6.69 (d, J = 15.3 Hz, 1H), 4.47 (t, J = 7.5 Hz, 2H), 4.00 (s, 3H), 2.74 (m, 4H), 2.04-1.86 (m, 4H), 1.84 (s, 6H), 1.11 (t, 3H). ^{13}C NMR of HXPI-E (75 MHz, CD_3OD; Fig. S8) δ 180.6, 170.7, 165.2, 160.5, 158.4, 147.5, 143.9, 142.8, 132.2, 131.1, 130.4, 129.2, 129.1, 124.0, 116.4, 116.3, 114.8, 111.7, 107.3, 104.5, 53.36, 52.59, 30.08, 28.14, 25.06, 22.56, 21.50, 11.61, 9.29. HR-ESI-MS: *m/z* calcd for $[C_{30}H_{32}NO_4]^+$, 470.2326; found, 470.2323 (Fig. S9).

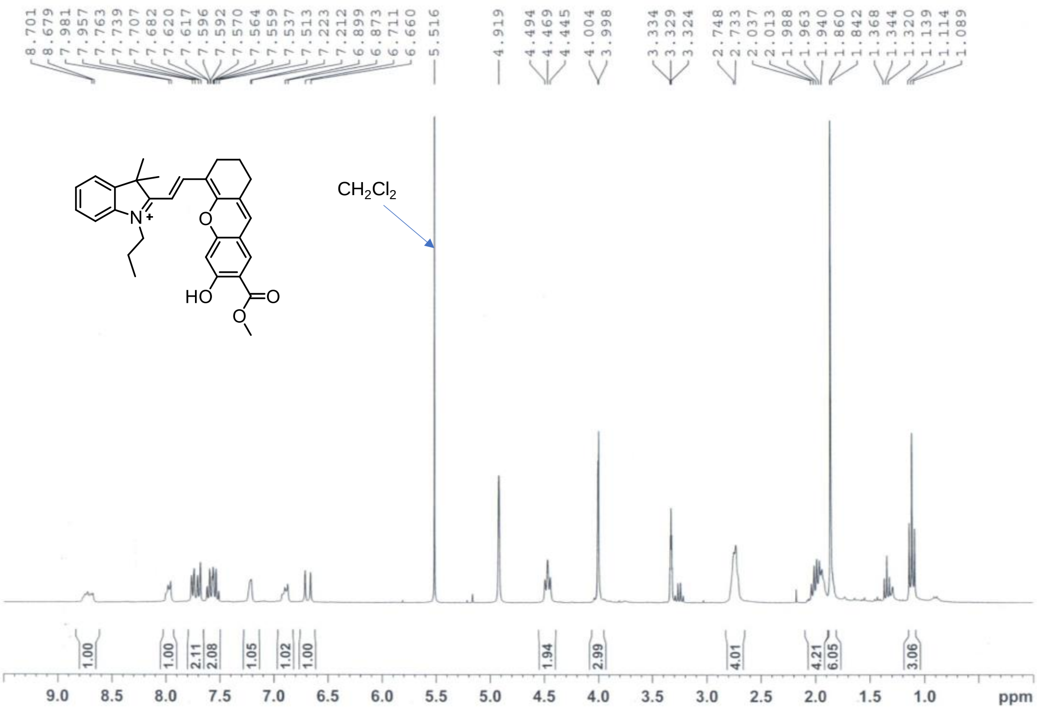

Fig. S7 ^{1}H NMR spectrum of HXPI-E (300 MHz, CD_3OD, 298 K)

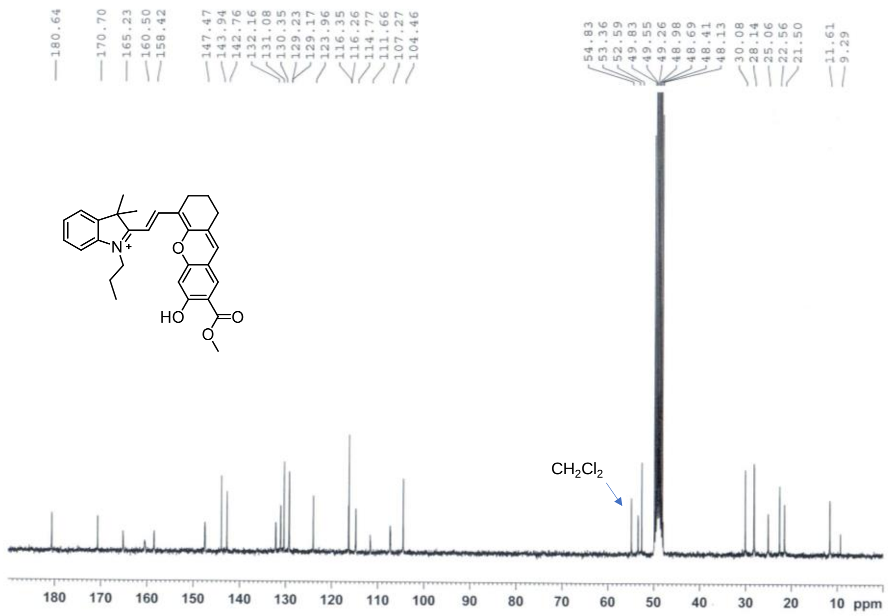

Fig. S8 ^{13}C NMR spectrum of HXPI-E (75 MHz, CD_3OD, 298 K).

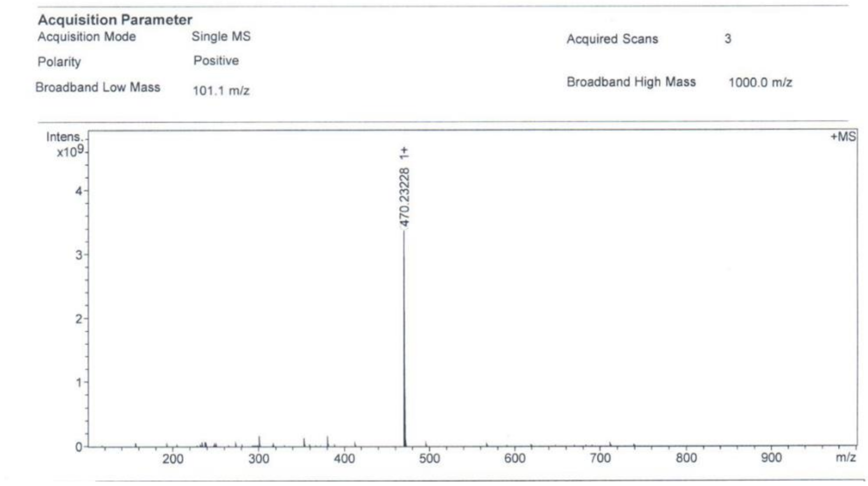

Fig. S9 HR-ESI-MS of HXPI-E.

3 Determination of octanol-water partition coefficient

The 1-octanol-water partition coefficient (Log P_{oct}) was calculated according to a reported procedure (Jung et al, *J. Am. Chem. Soc.* **2017**, *139*, 7595). The log P_{oct} values for HXPI-P were found to be 0.76 as noted in the main text.

4 General procedure for polarity measurement

Stock solution (1.0 mM) of HXPI-P was prepared in DMSO. For spectroscopic measurement, 30 μL stock solution of the probe was well mixed with 3.0 mL common solvents respectively, and then the mixture was transferred to a 1-cm quartz cell to measure absorbance against the corresponding reagent blank or fluorescence spectra with λ_{ex} = 635 nm.

5 Establishment of the polarity calibration curve

A series of solutions with different polarity were prepared by mixing 1,4-dioxane and water at varied volume ratios. 30 μL stock solution of the probe was added into 3.0 mL of the mixed solutions and fluorescence spectra were collected with λ_{ex} = 635 nm. A calibration curve was plotted by the emission maximum shifts or the fluorescence intensity ratios at two wavelengths against the dielectric constant of the mixed system.

6 Computational method

All the theoretical calculations were carried out with the density-functional theory (DFT) and time-dependent density-functional theory (TD-DFT) methods in Gaussian 09 package. Both the geometry optimization of ground state and first excited state were performed at the B3LYP method (Lee et al, *Phys. Rev. B*. **1988**, *37*, 785) with 6-31+G (d) basis set (McLean et al, *J. Chem. Phys.* **1980**, *72*, 5639) in the PCM solvent continuum models (Water and Dioxane; Cancès et al, *J. Chem. Phys.* **1997**, *107*, 3032). The vibration frequency calculations were carried out at the same computational method and basis set to make sure that the optimized structures were true energy minima. Based on the final optimized structures of ground state and first excited state, the dipole moment were also calculated at the same computational method and basis set.

7 Culture of Cells

HeLa, HepG2 and L-O2 cells were cultured using DMEM media. HFL-1 cells were propagated in Ham's F12k media. The media were all supplemented with 10% (v/v) fetal bovine serum (FBS, GIBCO) and 1% (v/v) penicillin-streptomycin. Cells were grown in a humidified 5% CO_2 incubator at 37 °C.

8 Cytotoxicity Assay.

The cytotoxicity of HXPI-P to HeLa cells was examined by standard MTT assay according to the previous report (Wan et al, *Angew. Chem. In. Ed*. **2014**, *53*, 10916).

9 Intracellular Fluorescence Imaging.

Cells were seeded in 15 mm glass-bottom culture dishes for 24 h to adhere before experiments. Before use, the cells were washed with FBS-free media for three times. For imaging, the cells were incubated with 5.0 μM HXPI-P in incubator for 10 min and then the cells were subjected to fluorescence imaging experiments using a 100× or 60× oil immersion objective lens. The pixel intensity in each fluorescence image was measured and averaged from at least five cells.

10 Co-localization Experiments

Cells (HeLa and HFL-1) seeded in glass-bottom culture dishes were simultaneously incubated with HXPI-P (2.0 μM) and Mito Green (500 nM)/ DND-26 (1.0 μM)/ ER Green (1.0 μM) for 10 min in media without FBS. The cells images were obtained with excitations at either 635 nm (for HXPI-P) or 488 nm (for Mito Green, DND-26 and ER Green); the corresponding fluorescence emissions were collected at 650-750 nm (for HXPI-P) and 500-550 nm (for Mito Green, DND-26 and ER Green), respectively.

11 Supplementary Figures

Table S1. Photo-physical properties of HXPI-P in various solvents at 25 ^{o}C.

HXPI-P (Solvent)	λ_{abs}[a] /nm	$\varepsilon_{max}(M^{-1}cm^{-1})$	λ_{em}[b] /nm	φ[c]	stocks Shift/nm
Water	648	17100	672	0.02	24
ethylene glycol	662	59900	694	0.19	32
MeOH	662	67200	710	0.14	48
EtOH	670	76600	715	0.29	45
1-butanol	676	94800	717	0.45	41
DCM	702	118700	730	0.98	28
diethyl ether	714	88700	735	0.49	21
1,4-dioxane	708	94500	733	0.73	25

[a]The maximal absorption of the dye. [b]The maximal emission of the dyes. [c] φ is the relative fluorescence quantum yield estimated by using indocyanine green (ICG, φ = 0.13 in DMSO) as a fluorescence standard (Reindl et al, *J. Photochem. Photobiol. A: Chem.* **1997**, *105*, 65).

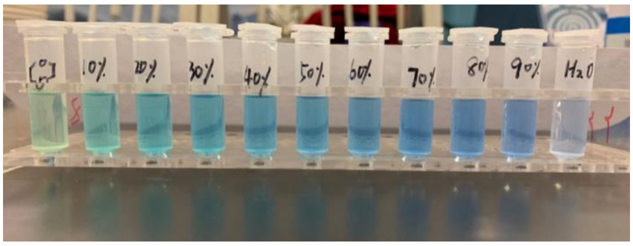

Fig. S10 Color changes of HXPI-P (10 μM) in the mixture of water and 1,4-dioxane. The percentage indicates the volume fraction of water.

$$hc\tilde{\nu}_{max} = -\frac{2\mu_e(\mu_e-\mu_g)}{\alpha^3}\Delta f + \text{constant} \quad \text{(Equation S1)}$$

Equation S1 is the Lippert-Metaga equation, which neglects the mean solute polarizability in the excited and ground states (Singh et al, Photochem. Photobiol. 1998, 68, 32). Here, h is the Plank constant, c is the light speed in vacuum, $\tilde{\nu}_{max}$ is the solvent-equilibrated fluorescence maxima (wave number), μ_e and μ_g are the dipole moments of excited and ground states, α is the Onsager cavity radius, Δf is the orientational polarizability of solvents, and $\Delta f = \frac{\varepsilon-1}{2\varepsilon+1} - \frac{n^2-1}{4n^2+2}$ (ε is the solvent dielectric constant, and n is the solvent refractive index). Generally speaking, Δf is positively correlated to the dielectric constant ε. As can be seen from Fig. 1C and Fig. 2C, $\tilde{\nu}_{max}$ will increase in solvents with higher polarity. Therefore, the slope of Equation S1 is positive. That is to say, there is a decrease in the dipole moment upon excitation. In such cases, the ground state will be energetically stabilized with respect to the excited state, and hence, a significant blue shift of the fluorescence will be observed in high polarity solvents.

Table S2. Theoretical calculation for the dipole moments of HXPI-P in water and 1,4-dioxiane from B3LYP functional with 6-31+G (d) basis.

Solvent	State	X	Y	Z	μ (D)
Water	Ground State	6.4024	4.9759	0.8184	8.1498
Water	First Excited State	3.3411	5.6043	1.1249	6.6209
Dioxane	Ground State	5.2634	4.0294	0.8032	6.6771
Dioxane	First Excited State	2.5029	4.5243	0.9423	5.2556

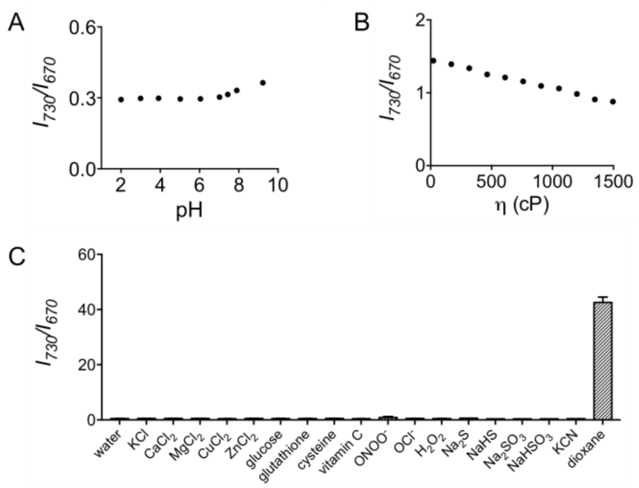

Fig. S11 Fluorescence response of HXPI-P (10 μM) to pH, viscosity and various biological coexisting substances. (A) Plot of I_{730}/I_{670} *vs* pH in the range of pH 2.0 to pH 9.2. (B) Plot of I_{730}/I_{670} *vs* viscosity in the range of η = 22.1 (glycol) to η = 1495 (glycerol). (C) Fluorescence response to various substances: water, KCl (150 mM), $CaCl_2$ (2.0 mM), $MgCl_2$ (2.0 mM), $CuCl_2$ (100 μM), $ZnCl_2$ (100 μM), glucose (10 mM), glutathione (1.0 mM), cysteine (100 μM), vitamin C (1.0 mM), $ONOO^-$ (100 μM), OCl^- (100 μM), H_2O_2 (100 μM), Na_2S (100 μM), NaHS (100 μM), Na_2SO_3 (100 μM), $NaHSO_3$ (100 μM), KCN (100 μM) and 1,4-dioxane. λ_{ex} = 635 nm. Data are expressed as the mean ± SD of three separate measurements.

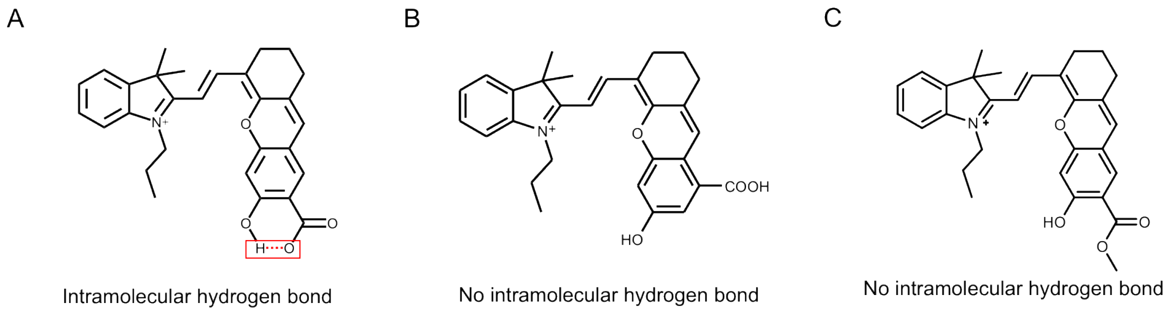

Fig. S12 Structures of (A) probe HXPI-P, (B) control compound HXPI-M and (C) control compound HXPI-E.

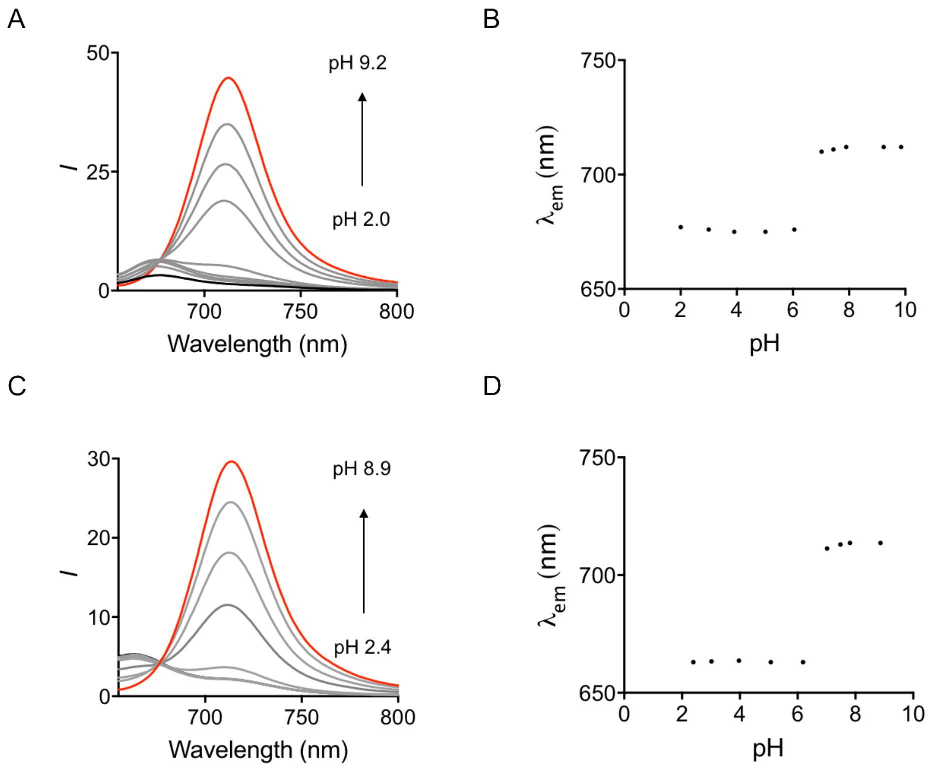

Fig. S13 Fluorescence responses of HXPI-M and HXPI-E (10 μM) to pH. (A) Fluorescence emission spectra of HXPI-M in phosphate buffer (20 mM) at different pH values. (B) Plot of λ_{em} vs pH of HXPI-

M in the range of pH 2.0 to pH 9.2. (C) Fluorescence emission spectra of HXPI-E in phosphate buffer (20 mM) at different pH values. (D) Plot of λ_{em} vs pH of HXPI-E in the range of pH 2.4 to pH 8.9. The percentage indicates the volume fraction. λ_{ex} = 635 nm. Data are expressed as the mean ± SD of three separate measurements.

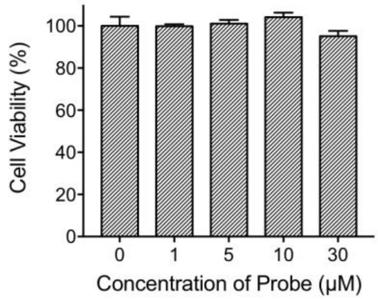

Fig. S14 Cell viability of HeLa cells treated with HXPI-P at varied concentrations for 24 h. The results are the mean ± SD of five separate measurements.

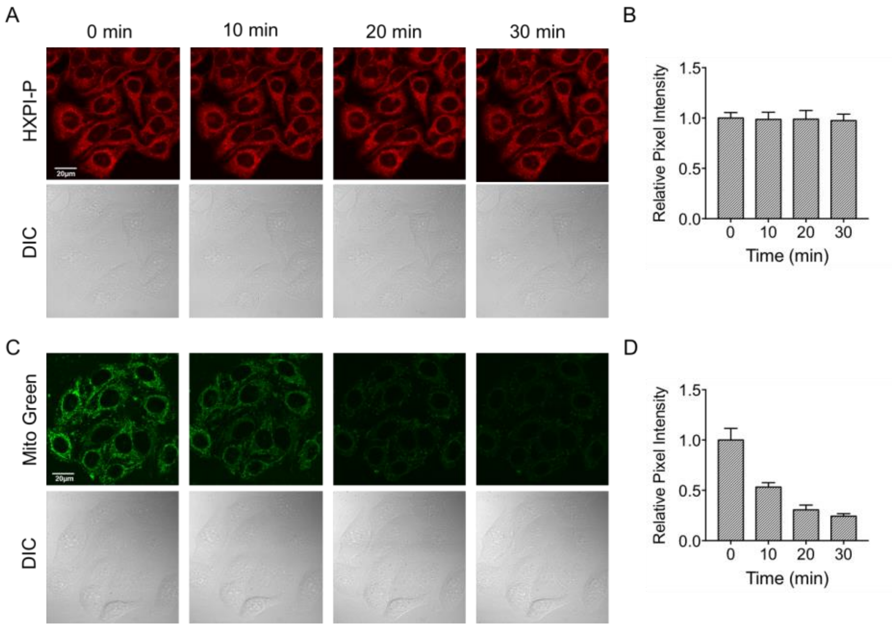

Fig. S15 Photostability comparison of HXPI-P and Mito Green in HeLa cells. (A) Images of HeLa cells stained with HXPI-P (5.0 μM, λ_{ex} = 635 nm, λ_{em} = 650-750 nm). (B) Changes of fluorescence intensity of HXPI-P in cells. (C) Images of HeLa cells stained with Mito Green (500 nM, λ_{ex} = 488 nm, λ_{em} = 500-550 nm). (D) Changes of fluorescence intensity of Mito Green in cells. The initial fluorescence intensity (i.e., at about 0 min) is defined as 1.0. The data are expressed as the mean ± SD of three separate measurements. Fluorescence imaging was performed under the continual excitations of 635 or 488 nm for different periods of time (0-30 min). Light power density: 2.0 mW/cm^2. Scale bars, 20 μm.

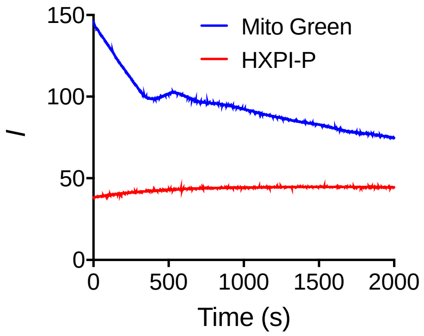

Fig. S16 Photostability of HXPI-P (5.0 μM, $\lambda_{ex/em}$ = 635/670 nm) and Mito Green (500 nM, $\lambda_{ex/em}$ = 488/520 nm) in water under continuous irradiation of xenon lamp (150 W).

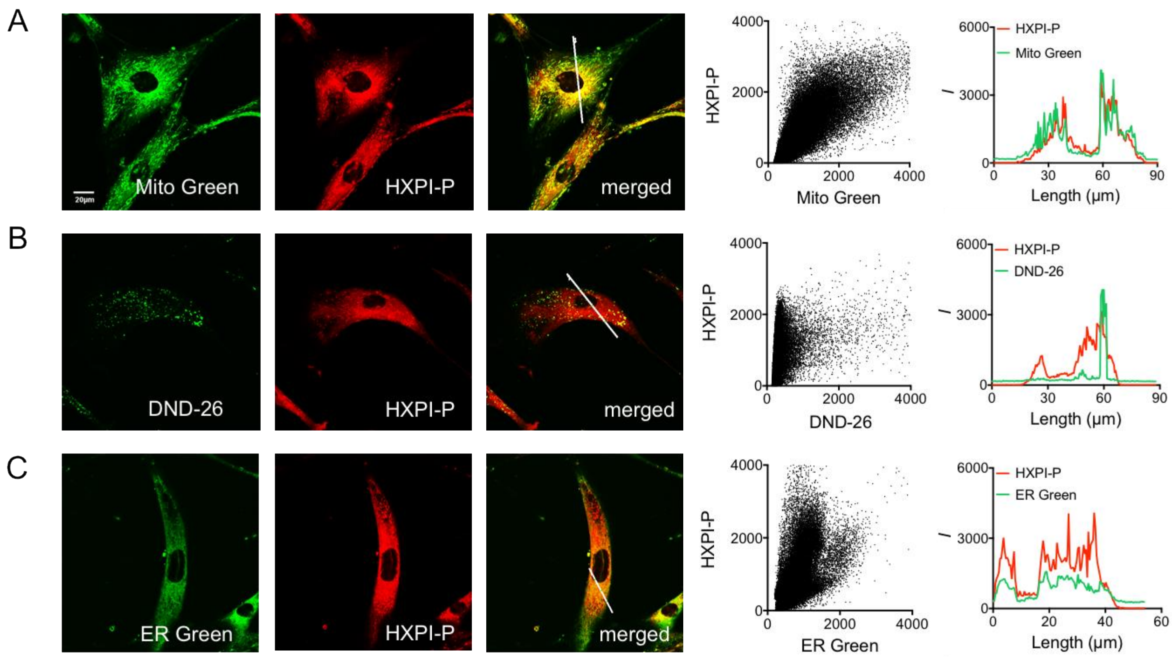

Fig. S17 Mitochondria-targeting properties of HXPI-P in HFL-1 cells. (A) Colocalization images of HFL-1 cells stained with Mito Green (500 nM, green channel, λ_{ex} = 488 nm, λ_{em} = 500-550 nm) and HXPI-P (2.0 μM, red channel, λ_{ex} = 635 nm, λ_{em} = 650-750 nm), and the correlation of HXPI-P and Mito Green intensities as well as the intensity profiles within the ROI (white line in the merged image of A; Pearson's coefficient 0.90). (B) Colocalization images of HFL-1 cells stained with DND-26 (1.0 μM, green channel, λ_{ex} = 488 nm, λ_{em} = 500-550 nm) and HXPI-P [as in (A)], and the correlation of HXPI-P and DND-26 intensities as well as the intensity profiles within the ROI (white line in the merged image of B; Pearson's coefficient 0.54). (C) Colocalization images of HFL-1 cells stained with ER Green (1.0 μM, green channel, λ_{ex} = 488 nm, λ_{em} = 500-550 nm) and HXPI-P [as in (A)], and the correlation of HXPI-P and ER Green intensities as well as the intensity profiles within the ROI (white line in the merged image of C; Pearson's coefficient 0.80). Scale bar = 20 μm.

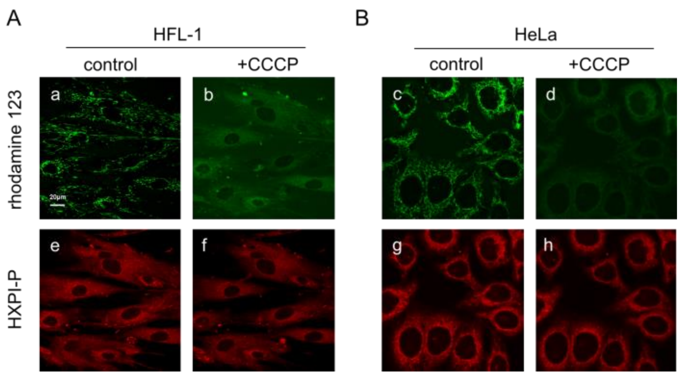

Fig. S18 Mitochondria-targeting properties of HXPI-P in depolarized HFL-1 and HeLa cells. Cells were treated with HXPI-P (2.0 μM) and rhodamine 123 (500 nM) for 10 min (control); the probe and rhodamine 123 treated cells were subjected to CCCP (100 nM) for 5 min to induce mitochondria uncoupling. First row, rhodamine 123 channel (λ_{ex} = 488 nm, λ_{em} = 500-550 nm); second row, HXPI-P channel (λ_{ex} = 635 nm, λ_{em} = 650-750 nm). Scale bar = 20 μm.

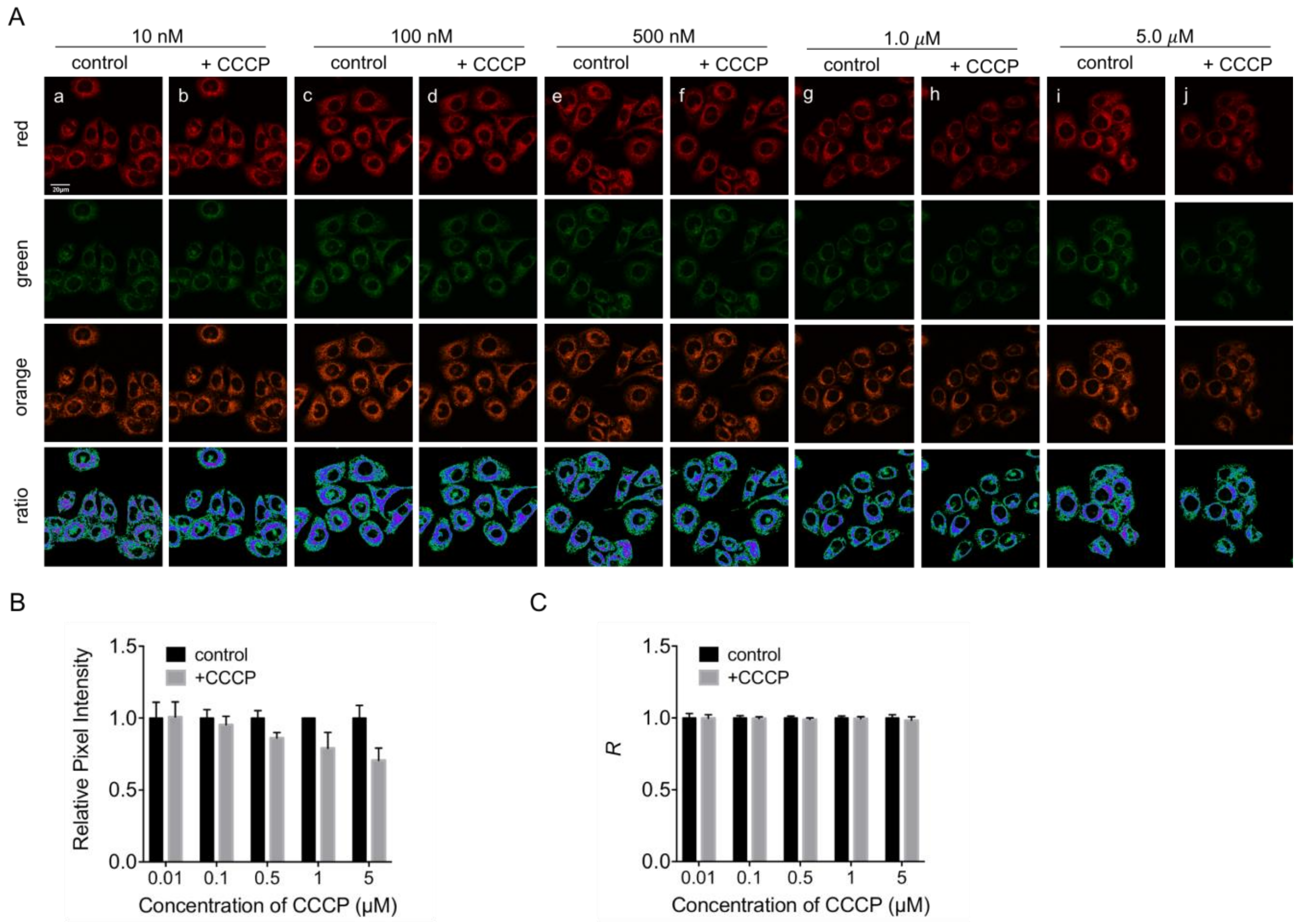

Fig. S19 MMP effects on the fluorescence intensity of HXPI-P in HeLa cells. Cells were treated with HXPI-P (5.0 μM) for 10 min (control); the probe-treated cells were then subjected to different concentrations of CCCP for 5 min to induce mitochondria uncoupling. Red channel (λ_{em} = 650-750 nm); green channel (λ_{em} = 655-685 nm); orange channel (λ_{em} = 700-730 nm); the fourth row shows the ratiometric images between orange and green channels. λ_{ex} = 635 nm. Scale bar = 20 μm. (B) Relative pixel intensity of the fluorescence images a-j in panel (A). (C) Relative fluorescence intensity ratios (R) of the corresponding ratio images in panel (A). The pixel intensity and the relative ratio values from the control images are defined as 1.0.

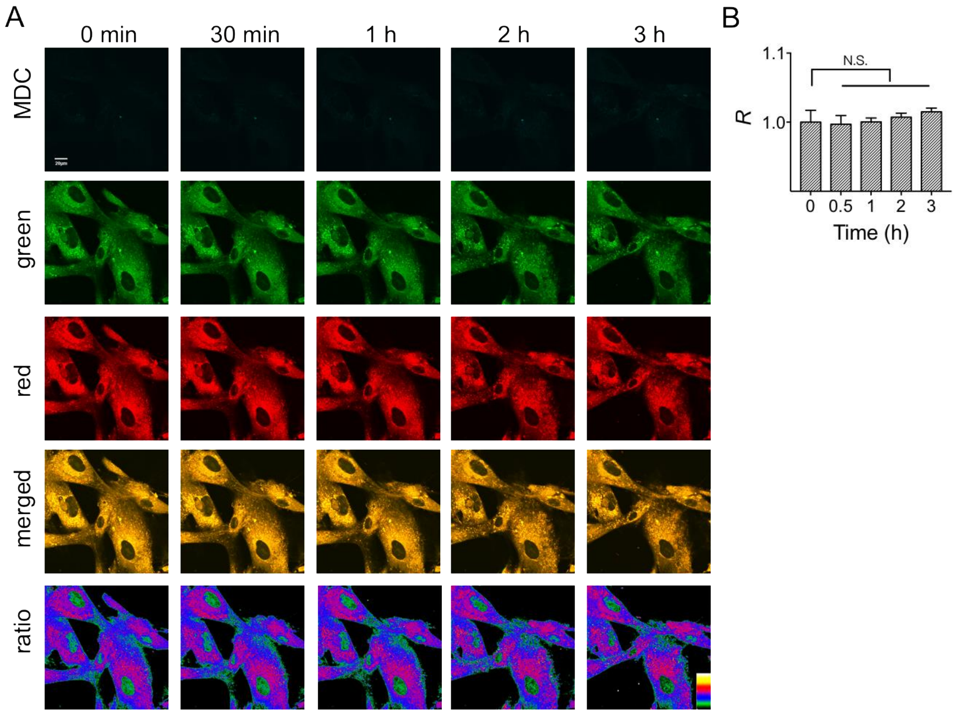

Fig. S20 Confocal fluorescence images of HFL-1 cells incubated with chloroquine (10 μM), HXPI-P (5.0 μM) and MDC (1.0 μM). (A) MDC (λ_{em} = 450-550 nm) channel was collected at λ_{ex} = 405 nm, green (λ_{em} = 655-685 nm) and red (λ_{em} = 700-730 nm) channels were collected at λ_{ex} = 635 nm. The images in the third row are the merged ones of red and green channels. The forth row shows the corresponding ratiometric images between red and green channels Scale bar = 20 μm. (B) Polarity changes of mitochondria with time. The fluorescence intensity ratio at 0 min is defined as 1.0. The data are expressed as the mean ± SD of three measurements. Significant differences are performed by Student's t-test.

Table S3. Molecule coordinates of HXPI-P

Ground State, Water:

Number	Atomic Number	X	Y	Z
1	6	5.074943	-0.146510	-0.315753
2	6	6.456033	-0.133154	-0.471213
3	6	7.145117	-1.355347	-0.485201

4	6	6.454218	-2.565288	-0.343597
5	6	5.062767	-2.589882	-0.187151
6	6	4.402366	-1.362301	-0.180471
7	7	3.015761	-1.105323	-0.049283
8	6	2.040422	-2.187818	0.144275
9	6	1.807648	-2.511646	1.627906
10	6	0.838766	-3.685230	1.806848
11	6	2.749949	0.219033	-0.076757
12	6	1.437367	0.720524	0.037782
13	6	1.117380	2.073360	0.042726
14	6	4.071540	0.991385	-0.253742
15	6	4.383717	1.895354	0.967926
16	6	4.095553	1.800018	-1.576044
17	6	-2.550975	4.360284	0.561854
18	6	-1.341850	4.973055	-0.149486
19	6	-0.061939	4.261934	0.294404
20	6	-0.128457	2.741648	0.150085
21	6	-1.391009	2.145257	0.142762
22	6	-2.622757	2.871383	0.315274
23	6	-3.809862	2.196226	0.258770
24	6	-3.852321	0.781491	0.037598
25	6	-2.625738	0.107526	-0.122666
26	8	-1.447339	0.790728	-0.057642
27	6	-2.562646	-1.259253	-0.354703
28	6	-3.745490	-2.002889	-0.425818
29	8	-3.704025	-3.333600	-0.655808
30	6	-5.007818	-1.360961	-0.262732
31	6	-5.025932	0.019774	-0.037333
32	6	-6.286316	-2.112167	-0.324608
33	8	-6.414084	-3.316376	-0.473083
34	8	-7.366670	-1.300033	-0.191797
35	1	6.999983	0.801192	-0.580010
36	1	8.224600	-1.362388	-0.605145
37	1	7.001574	-3.503432	-0.353019
38	1	4.539671	-3.533142	-0.073570
39	1	2.770664	-2.748612	2.096481
40	1	1.220388	-4.593375	1.324590
41	1	-0.145422	-3.462433	1.377846
42	1	0.696780	-3.905118	2.870510
43	1	1.418427	-1.619949	2.134244
44	1	2.422759	-3.062667	-0.387423
45	1	1.111224	-1.905214	-0.354099
46	1	0.639527	0.000634	0.142398

47	1	1.950086	2.765618	-0.015346
48	1	4.342711	1.323737	1.900489
49	1	3.690430	2.736081	1.047935
50	1	5.394131	2.302442	0.860364
51	1	3.876167	1.156230	-2.433782
52	1	5.092575	2.230000	-1.715814
53	1	3.372278	2.619218	-1.566267
54	1	-2.463630	4.541814	1.643362
55	1	-3.486848	4.827441	0.237491
56	1	-1.272672	6.042474	0.077283
57	1	-1.464598	4.876512	-1.236595
58	1	0.791629	4.633532	-0.284216
59	1	0.145874	4.516721	1.344668
60	1	-4.746225	2.734222	0.383439
61	1	-1.601260	-1.743686	-0.486903
62	1	-2.781248	-3.627504	-0.749549
63	1	-5.979192	0.520328	0.084543
64	1	-8.161841	-1.864025	-0.237894

First Excited State, Water:

Number	Atomic Number	X	Y	Z
1	6	5.039673	-0.194715	-0.364484
2	6	6.409542	-0.229966	-0.576341
3	6	7.066441	-1.471705	-0.565544
4	6	6.348952	-2.659073	-0.340385
5	6	4.970902	-2.642212	-0.125618
6	6	4.330384	-1.392675	-0.145626
7	7	2.983459	-1.104312	0.025928
8	6	1.984046	-2.136277	0.311584
9	6	1.785167	-2.376783	1.818405
10	6	0.758225	-3.483581	2.079687
11	6	2.742692	0.257786	-0.054420
12	6	1.464358	0.787218	0.076713
13	6	1.135516	2.165961	0.035810
14	6	4.076404	0.976158	-0.310405
15	6	4.468046	1.921040	0.858874
16	6	4.077895	1.741828	-1.660005
17	6	-2.584822	4.351960	0.584498
18	6	-1.390553	4.998163	-0.121759
19	6	-0.095285	4.306295	0.308874
20	6	-0.112414	2.794116	0.136306
21	6	-1.402518	2.178367	0.124643

22	6	-2.614004	2.862939	0.335349
23	6	-3.817503	2.159422	0.300710
24	6	-3.831776	0.765754	0.046918
25	6	-2.585821	0.119571	-0.185434
26	8	-1.427184	0.821602	-0.138480
27	6	-2.506370	-1.233828	-0.473830
28	6	-3.675815	-2.003774	-0.530513
29	8	-3.612923	-3.321438	-0.804820
30	6	-4.949327	-1.398811	-0.297583
31	6	-4.993299	-0.030677	-0.016998
32	6	-6.209433	-2.181166	-0.349652
33	8	-6.315498	-3.371110	-0.599633
34	8	-7.298750	-1.416321	-0.081007
35	1	6.973822	0.682463	-0.748394
36	1	8.138999	-1.514855	-0.730610
37	1	6.874580	-3.609584	-0.331491
38	1	4.430511	-3.565437	0.052202
39	1	2.749458	-2.646132	2.266512
40	1	1.075756	-4.434540	1.634506
41	1	-0.222483	-3.225340	1.662289
42	1	0.632399	-3.643172	3.156206
43	1	1.462649	-1.441666	2.292011
44	1	2.311996	-3.054604	-0.182322
45	1	1.044674	-1.846728	-0.165151
46	1	0.655336	0.090050	0.242406
47	1	1.961633	2.864055	-0.036243
48	1	4.454446	1.388347	1.814969
49	1	3.794853	2.778747	0.932221
50	1	5.481045	2.301784	0.691749
51	1	3.815524	1.075799	-2.488131
52	1	5.077761	2.147407	-1.847564
53	1	3.370666	2.575210	-1.650616
54	1	-2.514746	4.535484	1.667344
55	1	-3.531481	4.791899	0.252737
56	1	-1.339035	6.064814	0.121494
57	1	-1.516025	4.916652	-1.209621
58	1	0.761424	4.715887	-0.238017
59	1	0.089554	4.528558	1.372555
60	1	-4.755653	2.684433	0.457236
61	1	-1.539885	-1.690537	-0.660221
62	1	-2.687847	-3.594273	-0.937228
63	1	-5.952856	0.441324	0.156416
64	1	-8.082265	-1.995734	-0.135896

Ground State, Dioxane:

Number	Atomic Number	X	Y	Z
1	6	5.045452	-0.168017	-0.396297
2	6	6.415656	-0.178268	-0.627710
3	6	7.091877	-1.406957	-0.621777
4	6	6.400753	-2.600722	-0.383150
5	6	5.020710	-2.602219	-0.148270
6	6	4.372217	-1.368823	-0.165382
7	7	2.995863	-1.089977	0.027973
8	6	2.022920	-2.147104	0.330210
9	6	1.872446	-2.408387	1.836571
10	6	0.863774	-3.527719	2.115396
11	6	2.739101	0.235869	-0.052991
12	6	1.437270	0.751748	0.088855
13	6	1.112195	2.104768	0.062646
14	6	4.057040	0.983479	-0.330544
15	6	4.439557	1.931407	0.837049
16	6	4.016284	1.741723	-1.681230
17	6	-2.578420	4.346498	0.606763
18	6	-1.378679	4.980755	-0.102445
19	6	-0.088498	4.281503	0.331434
20	6	-0.136496	2.761406	0.176701
21	6	-1.394932	2.150413	0.162044
22	6	-2.632788	2.858856	0.345277
23	6	-3.812228	2.166931	0.284598
24	6	-3.840122	0.757844	0.038834
25	6	-2.607138	0.102651	-0.143313
26	8	-1.435869	0.799196	-0.061546
27	6	-2.529749	-1.256649	-0.414582
28	6	-3.706215	-2.011677	-0.500256
29	8	-3.660345	-3.330000	-0.773789
30	6	-4.973770	-1.388078	-0.307730
31	6	-5.007413	-0.017525	-0.048417
32	6	-6.244193	-2.162953	-0.378576
33	8	-6.345361	-3.364553	-0.519503
34	8	-7.334604	-1.358856	-0.259180
35	1	6.961902	0.743107	-0.810700
36	1	8.162398	-1.432026	-0.801951
37	1	6.939612	-3.543495	-0.377738
38	1	4.497654	-3.533454	0.041906
39	1	2.851458	-2.672269	2.254543

40	1	1.171067	-4.469911	1.645228
41	1	-0.134558	-3.270861	1.738967
42	1	0.774492	-3.707334	3.191598
43	1	1.556378	-1.482094	2.332234
44	1	2.356464	-3.050419	-0.187567
45	1	1.064439	-1.869805	-0.115271
46	1	0.640129	0.040899	0.246136
47	1	1.941365	2.799475	-0.021980
48	1	4.435840	1.400639	1.794343
49	1	3.763220	2.786422	0.913973
50	1	5.449702	2.317491	0.667554
51	1	3.755981	1.068297	-2.503930
52	1	5.004314	2.164983	-1.888588
53	1	3.293447	2.561768	-1.666129
54	1	-2.492614	4.520600	1.689727
55	1	-3.519553	4.807003	0.287876
56	1	-1.322291	6.048816	0.132939
57	1	-1.503651	4.893096	-1.189925
58	1	0.758402	4.668597	-0.247650
59	1	0.120334	4.531989	1.382698
60	1	-4.754686	2.691788	0.421927
61	1	-1.563478	-1.726495	-0.573857
62	1	-2.741029	-3.617295	-0.904000
63	1	-5.967951	0.465364	0.089604
64	1	-8.120058	-1.935841	-0.307877

First Excited State, Dioxane:

Number	Atomic Number	X	Y	Z
1	6	5.031732	-0.221367	-0.384194
2	6	6.396304	-0.264214	-0.622389
3	6	7.049793	-1.507170	-0.610027
4	6	6.333617	-2.689937	-0.355032
5	6	4.961360	-2.665699	-0.112499
6	6	4.322460	-1.415162	-0.136094
7	7	2.979705	-1.120552	0.057311
8	6	1.975362	-2.133003	0.377409
9	6	1.734780	-2.295313	1.889320
10	6	0.648567	-3.336220	2.179422
11	6	2.741108	0.248509	-0.039780
12	6	1.472690	0.780004	0.098389
13	6	1.143322	2.167470	0.052583
14	6	4.076429	0.956472	-0.323681

15	6	4.494261	1.904849	0.833504
16	6	4.060337	1.713678	-1.677311
17	6	-2.576008	4.354955	0.569345
18	6	-1.378337	4.997493	-0.135703
19	6	-0.084444	4.311988	0.310067
20	6	-0.094977	2.797862	0.140261
21	6	-1.391370	2.179552	0.125292
22	6	-2.601234	2.862920	0.331995
23	6	-3.805016	2.155250	0.296269
24	6	-3.818022	0.763430	0.042043
25	6	-2.572598	0.120557	-0.193561
26	8	-1.412386	0.826085	-0.141437
27	6	-2.491438	-1.230566	-0.491504
28	6	-3.660986	-2.002136	-0.554712
29	8	-3.603961	-3.313833	-0.844724
30	6	-4.933598	-1.399377	-0.311490
31	6	-4.980245	-0.036781	-0.024036
32	6	-6.193050	-2.194565	-0.360948
33	8	-6.281637	-3.384720	-0.585970
34	8	-7.285982	-1.424439	-0.115736
35	1	6.960376	0.643881	-0.816788
36	1	8.118289	-1.556031	-0.796965
37	1	6.857518	-3.641137	-0.345315
38	1	4.423829	-3.586211	0.088059
39	1	2.676426	-2.589416	2.368608
40	1	0.915074	-4.319713	1.773245
41	1	-0.315020	-3.040362	1.745519
42	1	0.502962	-3.451572	3.258514
43	1	1.452018	-1.325323	2.315770
44	1	2.309787	-3.078547	-0.058276
45	1	1.045950	-1.867359	-0.136495
46	1	0.660825	0.089460	0.278381
47	1	1.975879	2.859757	-0.008659
48	1	4.490959	1.379753	1.793978
49	1	3.830661	2.769793	0.911992
50	1	5.508212	2.275696	0.650894
51	1	3.785828	1.044597	-2.498992
52	1	5.057291	2.117231	-1.883484
53	1	3.354444	2.548269	-1.664239
54	1	-2.516347	4.551907	1.650466
55	1	-3.520229	4.790889	0.224905
56	1	-1.330906	6.066541	0.097199
57	1	-1.497224	4.906400	-1.223490

58	1	0.775291	4.724956	-0.230108
59	1	0.087208	4.540049	1.374769
60	1	-4.744338	2.679187	0.450715
61	1	-1.524228	-1.684899	-0.685616
62	1	-2.684349	-3.588134	-1.002376
63	1	-5.942337	0.429229	0.153608
64	1	-8.064842	-2.010649	-0.161677